RSC Advances

PAPER

View Article Online
View Journal | View Issue

Cite this: *RSC Adv.*, 2015, **5**, 10081

Facile synthesis of monodisperse poly(MAA/EGDMA)/Fe_3O_4 hydrogel microspheres with hollow structures for drug delivery systems: the hollow structure formation mechanism and effects of various metal ions on structural changes†

Seong-Jin Park,‡[a] Hyung-Seok Lim,‡[a] Young Moo Lee*[b] and Kyung-Do Suh*[a]

Received 5th November 2014
Accepted 6th January 2015

DOI: 10.1039/c4ra13904f

www.rsc.org/advances

This study presents a facile fabrication method for monodisperse poly(methacrylic acid/ethylene glycol dimethacrylate)/Fe_3O_4 [poly(MAA/EGDMA)/Fe_3O_4] composite microcapsules with magnetic properties and hollow structures for use as a targeted drug delivery system. In aqueous solution, the iron ions diffuse into the negatively-charged spherical polymer particles by electrostatic attraction. Since the obtained polymer–metal complexes decrease the repulsive force between the negatively-charged carboxyl groups of the polymer chains, the chelating parts of the polymer particles lose their hydrophilic properties and become relatively hydrophobic. As the number of iron ions continues to increase in the polymer particles, an internal cavity begins to be formed by interaction between the hydrophobic domains and the inner polymer chains. After the reducing agent is added into the synthetic system, Fe_3O_4 nanoparticles formed in the shells of the polymer particles retain the hollow structure. Confocal laser scanning microscopy and zeta potential measurements are employed to confirm the formation of the hollow structure during the diffusion of the various metal ions into the polymer gel. The magnetic properties of the poly(MAA/EGDMA)/Fe_3O_4 composite microcapsules synthesized under diverse experimental conditions are characterized by a vibrating sample magnetometer. The controlled release behavior of the model drug doxorubicin hydrochloride from the polymer–metal hollow composite microcapsules is investigated under different pH conditions.

Introduction

Organic–inorganic hybrid materials have attracted extensive interest as smart materials in numerous fields including optics, electronics, ionics, mechanics, energy, environmental science, biology, medicine, material separation, functional smart coatings, fuel, solar cells, catalysts and sensors.[1] Specifically, these hybrid organic polymer materials containing various inorganic materials can respond to two or more stimuli and enhance the physical and mechanical properties of the original organic polymer.[2] Recently, the use of magnetite (Fe_3O_4) in composite hydrogels has attracted interest due to its prominent advantages of favorable magnetic properties, biocompatibility, biodegradability, low toxicity, chemical stability in a physiological environment, and potential applications in biomedical fields, especially in the field of targeted drug delivery. For example, Guo's research group reported on magnetic and pH-responsive nano-carriers with multilayer core–shells. These composites were synthesized by alkaline co-precipitation of ferric and ferrous ions in the presence of a tri-block copolymer.[3] In addition, ordered mesoporous silica microspheres with a silica-coated magnetite core prepared *via* a surfactant-templating approach were reported by Deng *et al.*[4] In particular, among the diverse magnetic hybrid materials used as targeted drug delivery systems, magnetic composites with hollow structures are compelling for diverse applications such as drug delivery systems, bio-encapsulation, medical diagnostics, catalysis, composite electronics and structural materials owing to their large inner cavities, high surface to volume ratios, and desirable drug-loading capacity.[5–7] Chatzipavlidis *et al.* evaluated hollow polymer microspheres with pH-responsiveness and magnetic properties. The magnetic composites were fabricated by two-stage distillation–

[a]*Department of Chemical Engineering, College of Engineering, Hanyang University, Seoul, Republic of Korea, 133-791. E-mail: kdsuh@hanyang.ac.kr*

[b]*WCU Department of Energy Engineering, Hanyang University, Seoul, Republic of Korea, 133-791. E-mail: ymlee@hanyang.ac.kr*

† Electronic supplementary information (ESI) available: OM images of synthetic process; XRD patterns; EDX profiles; SEM images; cross-sectional images of pure poly(MAA/EGDMA) microspheres and after adding iron ion solution; effect of reducing agent for hollow structure (STEM images and EDS elemental maps); CLSM images of pure microspheres in various pHs; effects of other metal ions for hollow structure. See DOI: 10.1039/c4ra13904f

‡ These authors contributed equally to this work.

precipitation polymerization, and the metal nanocrystals were grown on the hydrogel particle surface.[8] Magnetic dual-targeting polyelectrolyte hybrid hollow microspheres prepared *via* the layer-by-layer self-assembly technique were described by Du *et al.*[9] These synthetic methods require a step for the removal of the core through chemical etching and Soxhlet extraction. In our previous study, we suggested a facile method to prepare hollow poly(methacrylic acid/ethylene glycol dimethacrylate) [poly(MAA/EGDMA)] microcapsules by phase separation between water and hydrophobic polymer/surfactant complexes. The hydrophobic segments of the surfactants form complexes with the polymer chains as the positively-charged surfactants diffuse into the negatively-charged polymer particles by electrostatic attraction.[10] As a result, an interior cavity is formed by the phase separation between water and the complexes.

In the present study, we investigated the generation of an interior cavity in hydrogel microspheres using metal salts in aqueous solution with no need for removal of the microsphere core. First, poly(MAA/EGDMA) microspheres were synthesized by distillation–precipitation polymerization with ethylene glycol dimethacrylate as the cross-linker. The polymer gel forming a hollow structure was obtained through the diffusion of iron ions into the negatively-charged spherical polymer particles by electrostatic attraction. Polymer particles retain their hollow structures by virtue of the Fe_3O_4 nanocrystals formed by reducing agents. This facile one-pot synthetic method is very economical and safe, because no heating energy or chemical etching is needed to generate the hollow structure. The key point of our synthetic system is the use of the spherical hydrogel microspheres with the moderate degree of crosslinking. As the number of polymer–iron ion complexes increases in the outer parts of the polymer particles, the particle size decreased significantly, and at the same time the internal cavity is formed by the phase separation between the inner water phase and the hydrophobic domains of the polymer–iron ion complexes. This happens because the collapsed chains of moderate cross-linked networks in the inner part are pulled out toward the hydrophobic domains of the polymer–iron ion complexes by hydrophobic interactions. After the iron ions are reduced, the carboxylic groups in the outer part of the hydrogel network are chemisorbed onto the surfaces of the metal oxide nanoparticles *via* carboxylate bonding[11,12] and thus stabilize the hollow structure.

A schematic illustration of the synthetic system is given in Scheme 1. In order to generate the hollow structure, it is important to adjust the concentration of the metal precursor solution as well as the degree of crosslinking density of the hydrogel microspheres. The magnetic properties and controlled-release behaviors of the hollow poly(MAA/EGDMA)/Fe_3O_4 composite microcapsules were investigated using a magnetometer and doxorubicin as a model drug under different pH levels. In addition, the formation of metal oxide nanoparticles in the hydrogel matrix is the key to maintaining the hollow structures of the dried microspheres. This structural stability was examined using focused ion beam scanning electron microscopy (FIB-SEM), high-resolution transmission electron microscopy (HR-TEM), and confocal laser scanning microscopy (CLSM) under dried and dispersed conditions.

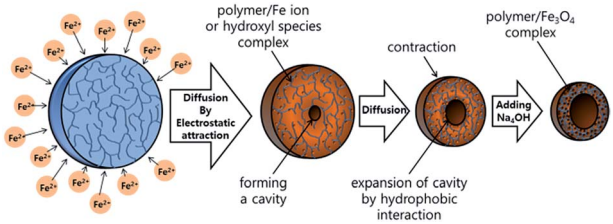

Scheme 1 Schematic illustration of the mechanism of formation of the poly(MAA/EGDMA)/Fe_3O_4 composite microcapsules with hollow structure.

Experimental section

Materials

Methacrylic acid (MAA, purity 99%, Sigma Aldrich) and ethyleneglycoldimethacrylate (EGDMA, TCI) were used without purification; α,α′-azobis(isobutyronitrile) (AIBN, Junsei) was recrystallized to remove an inhibitor from methanol before use. Sodium hydroxide (NaOH, purity 98+%, Aldrich), iron(II) chloride ($FeCl_2 \cdot 4H_2O$), and ammonium hydroxide (NH_4OH, ~28%, Daejung Chemical) were used as received. Distilled water (DI water) and acetonitrile (AN, Daejung Chemical) were used as solvents.

Preparation of monodisperse pH-responsive poly(MAA/EGDMA) microspheres

Poly(MAA/EGDMA) microspheres were synthesized by a distillation precipitation polymerization with EGDMA as the cross-linker. MAA (3.6 g) and EGDMA (0.4 g) were polymerized at 80 °C for 25 min without mechanical stirring in a medium consisting of AN (68 mL), DI water (12 mL), and AIBN (0.08 g) as an initiator. After 30 min of polymerization, the residual monomers were removed, and polymerized particles were isolated by centrifugation at 3600 rpm. The precipitates were washed three times with ethanol and water and then dried under vacuum.

Synthesis of hollow poly(MAA/EGDMA)/Fe_3O_4 hydrogel microspheres

Dried samples of the poly(MAA/EGDMA) microspheres (0.1 g) were added to distilled water (100 mL) and stirred for 2 h. The pH of the above solution containing swollen poly(MAA/EGDMA) microspheres was controlled up to 6.80 with the addition of 0.1 M NaOH solution, and the solution was stirred for a few hours. An aqueous solution of 0.0025 M iron(II) chloride was poured into the solution containing swollen poly(MAA/EGDMA) microspheres and stirred for 48 h at 200 rpm. The solution was then bubbled with N_2 for a few hours to remove oxygen in the solution. Then, ammonium hydroxide solution as a reduction agent was added under continuous mechanical stirring at 200 rpm.

Drug loading into poly(MAA/EGDMA)/Fe_3O_4 composite microcapsules

The loading amount of doxorubicin chloride (DOX) was obtained using the following approach: 10 mL of pH 7 buffer solution containing poly(MAA/EGDMA)/Fe_3O_4 hydrogel microspheres (0.01 g) was added into 10 mL of an aqueous solution containing DOX (1 mg). After being stirred for 24 h, the suspension was centrifuged and the supernatant was scanned at a wavelength of 485 nm using a UV spectrophotometer. The loading amount of DOX was calculated by comparing the scan results. In our system, the prepared poly(MAA/EGDMA)/Fe_3O_4 hydrogel microspheres showed loading efficiencies up to 84.6% of the total DOX.

In vitro drug release

DOX-loaded samples were washed with phosphate buffer saline (PBS, pH 7) to remove the residual free DOX. The sediment was dispersed in a buffer solution of 12 mL PBS (pH 7). The buffer solution containing the DOX-loaded samples was added to cellulose ester membrane tubes (molecular weight cut off = 14 000, Spectrum®), and the dialysis tubes were immersed in a reservoir filled with 47 mL of PBS at different pH levels (pH levels of 2, 4 and 7) and shaken moderately (240 rpm). At pre-determined times, 1 mL of the solution was collected from each reservoir, and the amounts of DOX released were analyzed by UV-visible spectrophotometry at 480 nm.

Characterization of poly(MAA/EGDMA)/Fe_3O_4 hydrogel microspheres

The processes for synthesizing the poly(MAA/EGDMA)/Fe_3O_4 hydrogel microspheres with hollow structures were characterized with optical microscopy (OM, B×51, Olympus). The confocal laser scanning microscope (I×70, Olympus) was utilized to analyze the morphological transition of the poly(MAA/EGDMA) hydrogel microspheres along with the molarity of the added iron ion solution. Fourier transform infrared spectroscopy (FT-IR, Magna IR-550, Nicolet) analysis was conducted to verify the chemical bonding components. Particle morphology was observed by scanning electron microscope (SEM, JSM-6300, JEOL). The size and structure of the poly(MAA/EGDMA)/Fe_3O_4 hydrogel microspheres were examined using a transmission electron microscope (TEM, JEM-2010, JEOL). Fe_3O_4 particles were confirmed by X-ray diffractometry (XRD). The Fe_3O_4 content of the obtained poly(MAA/EGDMA)/Fe_3O_4 hydrogel microspheres was calculated *via* thermogravimetric analysis (TGA, TG209F3, NETZSCH). The magnetic properties of the poly(MAA/EGDMA)/Fe_3O_4 hydrogel microspheres were studied with a vibrating sample magnetometer (VSM, Model #73002, Lake Shore) at room temperature. The release behavior of the model drug was characterized with a UV-vis spectrophotometer.

Results and discussion

The poly(MAA/EGDMA) microspheres were synthesized by distillation–precipitation polymerization. The synthesis mechanism for monodisperse poly(MAA/EGDMA) microspheres is occurred through an entropic distillation–precipitation polymerization manner. The capture of the oligomer radicals either by the adsorbed reactive vinyl group on the surface of PMAA nuclei or by the hydrogen-bonding interaction between the carboxylic acid on PMAA nuclei and carboxylic acid on oligomer radical in the solution may result in the growth of PMAA microspheres. Both the steric stabilization from the pendent chains and surface gel layer, and the electrostatic repulsion from the carboxyl acid groups prevent the particle coagulating leading to mono- or narrow-disperse PMAA microspheres.[13] The OM images in Fig. S1† show the synthetic steps for the monodisperse hollow poly(MAA/EGDMA)/Fe_3O_4 hydrogel microcapsules that are schematically illustrated in Scheme 1. First, the pH of an aqueous solution containing poly(MAA/EGDMA) hydrogel microspheres was adjusted from 4.5 to 6.8 by adding 0.1 M NaOH to completely ionize the carboxyl groups, as shown in Fig. S1a and b.† Then, as shown in Fig. S1c,† the poly(MAA/EGDMA) microspheres were fully contracted with addition of 0.0025 M ferrous chloride solution, because the electrostatic repulsion forces among the carboxyl groups of the matrix chains disappeared due to the screening of Fe^{2+} ions diffused in the hydrogel matrix. When NH_4OH solution was added as a reducing agent, the color of the suspension changed from light yellow to green and finally to dark brown after 48 h.

Fig. S2† shows the XRD patterns of the pure poly(MAA/EGDMA) microspheres and the composite microcapsules fabricated by adding different concentrations of iron(II) chloride. The pure poly(MAA/EGDMA) microspheres exhibited two broad peaks at 10° and 31°, as shown in Fig. S2a.† The peak intensities of the poly(MAA/EGDMA)/Fe_3O_4 composite microcapsules were decreased in contrast with those of the pure hydrogel microspheres due to the inorganic nanoparticles introduced into the polymer networks. In other words, since the polymer chains hindered the XRD of the inorganic nanoparticles, the crystalline patterns could not be confirmed clearly, as shown in Fig. S2b.†[14] Fig. S2c† shows that several peaks were observed as the concentration of iron(II) chloride increased. In order to verify the crystal types of the inorganic nanoparticles formed in the polymer phase, we prepared magnetite nanoparticles in the absence of polymer microspheres under the same experimental conditions and confirmed their diffraction patterns. The characteristic peaks of the pristine magnetic nanoparticles were $2\theta = 30.12°$, 35.48°, 43.12°, 57.02° and 62.62°, as indicated by their respective indices of (220), (311), (400), (511) and (440). The positions of the characteristic peaks of these particles correlate well with the standard values for the Fe_3O_4 phase (JCPDS number 88-0866). As a result, we conclude that magnetite nanocrystals were formed in the hydrogel networks. Fig. S3† shows the EDX (energy dispersive X-ray) profile of a poly(MAA/EGDMA)/Fe_3O_4 sample, in which the elements Fe (2.10 wt%), O (23.04 wt%), and C (74.86 wt%) were present.

The FT-IR spectra of the poly(MAA/EGDMA) microspheres and poly(MAA/EGDMA)/Fe_3O_4 microspheres are shown in Fig. 1a. Two samples have one broad peak at 3448 cm^{-1} and two

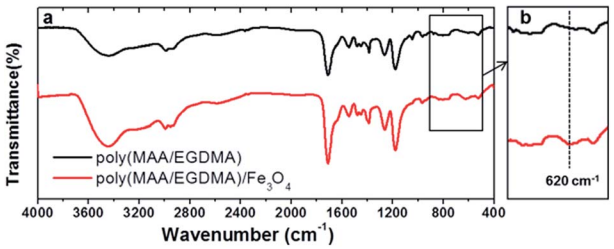

Fig. 1 FT-IR spectra of (black) poly(MAA/EGDMA) and (red) poly(MAA/EGDMA)/Fe_3O_4 composite microcapsules.

sharp peaks at 1473 and 1397 cm^{-1}, corresponding to the typical adsorption of the hydroxyl group and the methyl in the ester groups on MAA molecules. The absorption peaks at 1269 and 1171 cm^{-1} correspond to the C–O–C in the EGDMA molecules. Fig. 1b shows that the characteristic peak corresponding to the stretching vibration of the Fe–O bond was shifted to a higher wavenumber of 620 cm^{-1} compared to that of 570 cm^{-1} for the stretching mode of Fe–O in bulk Fe_3O_4,[15,16] indicating that the Fe_3O_4 was bound to the $-COO^-$ on the hydrogel surface.[17]

The samples obtained *via* the experimental procedures were examined by SEM. Fig. 2a shows pure poly(MAA/EGDMA) microspheres prepared by distillation–precipitation polymerization, which were easily collapsed by evaporating the water adsorbed in the hydrogel networks. The degree of particle cross-linking was not sufficient to maintain the spherical shape when the microspheres were completely dried. After iron ions were diffused into the hydrogel (Fig. 2b) and were reduced (Fig. 2c and d), sturdy spherical shapes with smooth particle surfaces were observed. This result indicates that the iron ions were well diffused into the hydrogel matrix rather than remaining in aqueous solution. Fig. S4a and b† show SEM images of the poly(MAA/EGDMA)/Fe_3O_4 composite microspheres fabricated under lower pH conditions (pH 4.8), which caused a weak ionization of the functional groups of the hydrogel matrix. As the electrostatic interactions between the carboxyl groups and iron ions decreased, the iron ions could not fully incorporate into the hydrogel matrix, and instead coated the surfaces of the poly(MAA/EGDMA) microspheres after the addition of a reducing agent.

The structural changes in poly(MAA/EGDMA) microspheres caused by increasing the concentration of iron(II) chloride solution were investigated using CLSM and FITC–dextran as a fluorescent dye. Fig. 3 shows CLSM images of the poly(MAA/EGDMA) microspheres with different concentrations of iron ion solution at pH 6.8. The pure poly(MAA/EGDMA) microspheres had a solid structure, as shown in Fig. 3a. As the 1.00×10^{-3} M iron ion solution was added into the suspension containing the hydrogel particles, the particle size of the poly(MAA/EGDMA) microspheres decreased from 4.2 μm to 3.8 μm because the cationic iron ions were adsorbed onto the surface and diffused into the negatively-charged polymer networks *via* electrostatic attraction. When the concentration of iron ions approached 2.50×10^{-3} M, the particle size decreased to 2.0 μm, and a doughnut-shaped dark shell appeared, as shown in Fig. 3c. In other words, the internal cavities appeared in the centers of the particles at around 2.50×10^{-3} M of iron ions. The line intensity profile shown in Fig. 3c was also changed compared to those in Fig. 3a and b. The structural changes in the poly(MAA/EGDMA) microspheres with various concentrations of the iron ion solution were also investigated by zeta potential measurements and size analysis. The zeta potentials and microsphere diameters were measured with respect to the increasing concentration of iron ions at room temperature, as shown in Fig. 3e (blue line and red line, respectively). The particle diameters decreased considerably from 3.8 to 2.3 μm with a stepwise increase in the concentration of iron ion solution from 1.00×10^{-3} to 2.00×10^{-3} M. In contrast, the zeta-potential values barely changed from −15.2 to −15.0 mV over the same concentration range of iron ion solution, as shown in Fig. 3e. As the concentration increased to 2.50×10^{-3} M, the particle size decreased slightly, while the zeta-potential value increased greatly from −15.0 to −12.7 mV. Thereafter, the zeta-

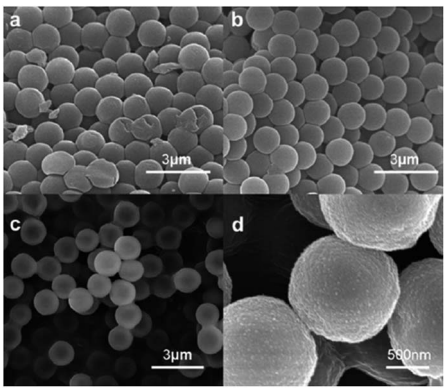

Fig. 2 SEM images of (a) pure poly(MAA/EGDMA), (b) poly(MAA/EGDMA)/iron ions microspheres and (c and d) poly(MAA/EGDMA)/Fe_3O_4 composite microcapsules at low magnification and high magnification.

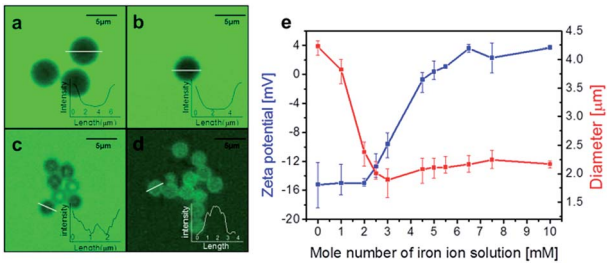

Fig. 3 CLSM images of the poly(MAA/EGDMA) microspheres after labeling the carboxyl groups with fluorescent dye (FITC–dextran, green color) dispersed in a pH 7 solution. The sequence was imaged upon increasing the $FeCl_2$ solution to adjust the concentration of $FeCl_2$: (a) without adding iron ions; (b) 1.00×10^{-3} M; (c) 2.50×10^{-3} M; (d) 5.00×10^{-3} M. Insets: fluorescent intensity profiles along the line through the microspheres indicating that the fluorescent intensity is observed in the cavity as well as the shell of the capsule. The scale bar represents 5 μm. (e) Zeta potential (Zetasizer nano ZS, blue line) and diameter (red line) of poly(MAA/EGDMA) microspheres with increasing $FeCl_2$ concentration.

potential values increased from −12.7 to −0.7 mV as the concentration increased to 4.50×10^{-3} M. From these data and the CLSM images, we demonstrated that the conformational transition of the poly(MAA/EGDMA) hydrogel microspheres is closely related to the diffusion of iron ions. As seen in the CLSM images, the poly(MAA/EGDMA) microspheres swollen in aqueous solution had a solid structure, and their average diameter and zeta-potential value were 4.2 μm and −15.2 mV, respectively. The hydrogel particles contracted when the iron ion solution was added to the particle suspension because the chelate complexes consisting of cationic iron ions and polymer chains with anionic functional groups were formed, inducing a hydrophobic interaction. The formation of an internal cavity was initiated from the center of each hydrogel microsphere by the hydrophobic interaction of the polymer–metal complexes toward the outer surface of the hydrogel microspheres. We verified that the molar concentration of 2.50×10^{-3} iron ions is the critical point where the internal cavity begins to form in the center of the particle by the phase separation between the chelate complexes and water. When more iron ions are added to the solution, the negatively-charged polymer networks cannot permit additional iron ions to diffuse into the gel particles because the electrostatic charge interaction between the metal ion and the negatively-charged polymer chain has reached the equilibrium state. As a result, iron ions were adsorbed onto the outer and inner surfaces of the particle shells, as shown in Fig. 3d. However, after the iron ions diffused into the hydrogel matrix, the cross-sectional images of dried poly(MAA/EGDMA) hydrogel microspheres exhibited solid structures (Fig. S5b†), which differed from the hollow structures seen in Fig. 3c. This result is attributed to the loss of electrical attraction caused by the evaporation of water in the poly(MAA/EGDMA)/Fe_3O_4 composite hydrogel matrix under vacuum conditions. In aqueous solution, since the hydrogel matrix has ionically cross-linked bonding and ionic bridges arising from the chelation of metal ions among the polymeric chains,[18] the internal cavity could be observed by CLSM. In contrast, the hollow structures of the composite microspheres were maintained even in a dry state after reducing agent was added to the particle suspension.

In order to observe the internal structure of the hollow poly(MAA/EGDMA)/Fe_3O_4 composite microcapsules, the prepared samples were dried and characterized using FIB-SEM and TEM. Fig. 4 shows the cross-sectional and TEM images of poly(MAA/EGDMA)/Fe_3O_4 composite microcapsules at low and high magnifications. All of the images clearly show that the composite microcapsules had a hollow structure. As mentioned above, this method does not require an extra processing step such as chemical etching to remove the core. As shown in Fig. S5a,† the pure poly(MAA/EGDMA) microspheres did not have a hollow structure; also, it is evident that the poly(MAA/EGDMA) microspheres were crushed by the ion beam used to produce the cross-sectional images in the FIB-SEM characterization. Fig. S6† shows scanning transmission electron microscopic (STEM) images and element distribution maps of poly(MAA/EGDMA)/Fe_3O_4 composite microspheres before and after addition of the reducing agent. The element distribution maps in Fig. S6a† indicate that the chelate complexes formed solely by ionic

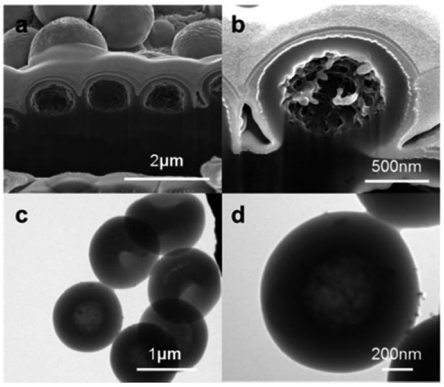

Fig. 4 (a and b) FIB-SEM and (c and d) TEM images of poly(MAA/EGDMA)/Fe_3O_4 composite microcapsules with hollow structure at (a and c) low magnification (b and d) high magnification.

interaction between the iron ions and ionized carboxyl groups of the hydrogel are non-permanent in contrast with the CTA(+)/hydrogel complexes.[10,19] However, all of the elements (C, Fe and O) comprising the composite microspheres after the iron ions have been reduced exist in the hollow structure, even in a dry state, as shown in Fig. S6b.† These results indicate that the Fe_3O_4 nanoparticles formed in the hollow hydrogel matrix have a large effect on the robust hollow structure.

Fig. S7† shows CLSM images of the poly(MAA/EGDMA) microspheres in aqueous solution at different pH levels. The average diameters of the poly(MAA/EGDMA) microspheres were 4.50, 4.02 and 2.46 μm at pH levels of 11 (Fig. S7a†), 5 (Fig. S7b†) and 2 (Fig. S7c†), respectively. The poly(MAA/EGDMA) microspheres were rapidly contracted in acidic aqueous solution due to the deionization of carboxyl groups, as shown in Fig. S7c.† As shown in Fig. 3c, the hydrogel microspheres dispersed in the iron ion solution were also contracted, but the pH value of the solution was not acidic (pH 6.45), unlike the solution without iron ions. Therefore, the contraction of the particles and the formation of the cavity can be attributed to the electrostatic attraction between the polymer chains and iron ions. The influence of crosslinking degree on the formation of hollow cavity in the poly(MAA/EGDMA) microspheres was confirmed by using the polymer particles with the different monomer ratios. Fig. S8† shows SEM and FIB-SEM images of the composite microcapsules with different monomer ratios; (a and b) 3.7 : 0.3, (c) 3.5 : 0.5 and (d) 3.4 : 0.6. In case of the EGDMA concentration of 7.5 wt% (3.7 : 0.3), the composite microcapsules are contracted because of their low degree of crosslinking, however the dry gels have a hollow cavity that can be seen through broken samples, as shown in Fig. S9b.† On the other hand, the FIB-SEM images of the composite microcapsules synthesized with higher amounts of EGDMA (12.5 and 15 wt%) show the solid structure without a hollow cavity, as shown in Fig. S9c and d.† These results indicate that the cross-linking degree is important factor to generate a hollow cavity in the polymer gel particle.

This synthetic method shows the feasibility of producing hollow composite microcapsules in the absence of a process step for the removal of the core. Fig. S9† exhibits CLSM images

of the hollow poly(MAA/EGDMA) microcapsules dispersed in $CuSO_4$, $FeCl_3$ and $SnCl_2$ aqueous solutions. All of the samples had hollow structures.

To investigate the amount of Fe_3O_4 nanoparticles introduced into the hydrogel microcapsules, TGA were conducted (Fig. 5). Both of the samples showed 15–20% weight loss in the temperature range between 50 and 300 °C, which is attributed to the loss of water and any physically absorbed materials. The TGA curve of the hollow poly(MAA/EGDMA)/Fe_3O_4 composite microcapsules, unlike that of the poly(MAA/EGDMA) hydrogel, indicates the onset of decomposition of organic polymers at a lower temperature, because the Fe_3O_4 nanoparticles weakened the interchain interactions and led to polymer decomposition.[20] The residues present after decomposition of the samples in N_2 at 900 °C were identified as Fe_3O_4. According to the residual mass, the content of Fe_3O_4 introduced in the poly(MAA/EGDMA)/Fe_3O_4 composite microcapsules was 7.63 wt%.

Characteristics of hollow poly(MAA/EGDMA)/Fe_3O_4 composite microcapsules

The magnetic properties of the hollow poly(MAA/EGDMA)/Fe_3O_4 composite microcapsules were evaluated by VSM at room temperature. Fig. 6a shows the magnetization curves of the hollow poly(MAA/EGDMA)/Fe_3O_4 composite microcapsules prepared with different concentrations (0.0025 M, 0.0030 M and 0.0040 M) of iron ion solution using $FeCl_2$. All of the samples displayed superparamagnetism, and the saturation magnetization (M_s) value was in direct proportion to the concentrations of the iron ion solution, 1.08, 2.36 and 3.49 emu g^{-1}, respectively. These M_s values are related to the amount of Fe_3O_4 nanoparticles introduced in the hollow hydrogel microcapsules. This result indicates that the magnetic intensity of the hollow hydrogel microcapsules can be easily adjusted as needed, and that these composite materials can be used for targeted drug delivery systems, especially in the presence of a magnetic field. We also confirmed the effect of medium pH, before adding iron ion solution, on the magnetic properties. Fig. 6b shows the M_s values of the hollow poly(MAA/EGDMA)/Fe_3O_4 composite microspheres fabricated under different pH values of medium before the iron ion solution was added; these results can be classified into three categories. First, in the experiment

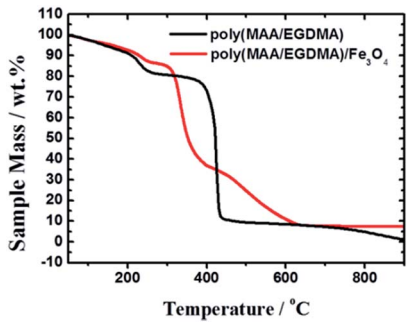

Fig. 5 TGA curves of poly(MAA/EGDMA)/Fe_3O_4 composite microcapsules with hollow structure and pure poly(MAA/EGDMA) hydrogel microspheres.

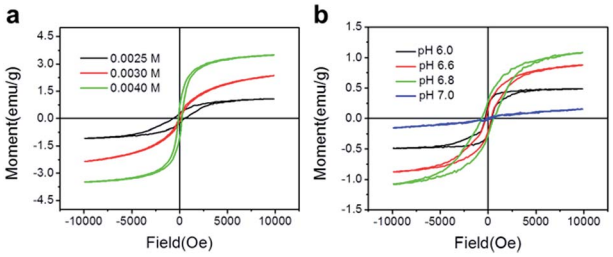

Fig. 6 VSM magnetization curves of poly(MAA/EGDMA)/Fe_3O_4 composite microspheres prepared in different (a) concentration of $FeCl_2$ (0.0025 M, 0.0030 M, 0.0040 M) and (b) pH values of aqueous solution during ion diffusion process.

performed without adjusting the pH of the medium, the composites exhibited a relatively high magnetization value (the maximum magnetization value was 6.50 emu g^{-1} at 10 kOe), because the composites prepared under low pH conditions were covered with iron oxide nanoparticles after the iron ions were reduced. This occurred because the iron ions could not diffuse into the hydrogel due to the lower ionization degree of the functional groups. This being so, the composites had the intrinsic magnetic properties of iron oxide. At a higher pH, the iron ions diffused into the hydrogel matrix, so that the iron oxides were inside the hydrogel rather than on the surface. The magnetization value of composites prepared under this experimental condition was lower than that of the composites prepared in an aqueous solution with a higher pH value. As shown in Fig. 6b, the magnetization value increased (0.48, 0.88, 1.08 emu g^{-1}) with increasing pH (6.0, 6.6, 6.8, respectively). However, the hollow poly(MAA/EGDMA)/Fe_3O_4 composite microspheres fabricated using pH 7 aqueous solution exhibited the lowest magnetization value because the iron ions reacted with the hydroxide in the medium before they diffused into the hydrogel matrix. The formed iron(III) hydroxides then precipitated and aggregated outside the hydrogel microspheres. Consequently, when the reducing agent was added, the goethites formed outside the hydrogel were only adsorbed by interaction with the hydrogel surface, and the magnetic intensity was diminished because the magnetic properties of goethite are weaker than those of magnetite.

In order to confirm the controlled loading and release capabilities, we used DOX as a model drug; DOX is one of the most effective cationic anticancer drugs, which is often used for the treatment of breast cancer, childhood solid tumors and soft tissue sarcomas. Owing to the development of tumor cells' resistance and cardiotoxicity, however, DOX is often limited. Therefore, a controlled-release DOX delivery system that can safely deliver the drug to the targeted tissue and selectively release the drug *via* the response to diverse stimuli, such as temperature or pH value could potentially be an effective way.[21–23] The hollow poly(MAA/EGDMA)/Fe_3O_4 composite microcapsules are appropriate as a targeted drug delivery system because of their biocompatibility, pH-responsiveness and magnetic properties. In these trials, pH was applied to control the loading and releasing of DOX as a model drug. The loading and release of DOX into the hollow poly(MAA/EGDMA)/

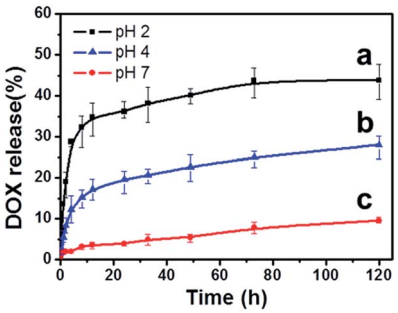

Fig. 7 Doxorubicin cumulative release from the hollow poly(MAA/EGDMA)/Fe_3O_4 composite microcapsules *versus* incubation time. Release profiles at different pH values (a) pH 2, (b) pH 4 and (c) pH 7.

Fe_3O_4 composite microcapsules is predominantly controlled by osmotic force. When hollow poly(MAA/EGDMA)/Fe_3O_4 composite microcapsules were dispersed in DI water, the composite microcapsules swelled, absorbing the external solvent. The external and internal states of the hydrogel became the same over time. However, if the pH of the solution dispersing the composites was changed, the mechanism influenced by the osmotic force would be interrupted by other effects. The pK_a values of poly(MAA) and DOX were about 5.5 and 8.6, respectively.[24] In the loading process of DOX in PBS solution of pH 7.0, most of the pendant carboxylic acid groups on the polymer chains were deprotonated to form carboxylate anions, whereas most of the DOX existed in protonated cationic form. Therefore, the DOX was well loaded in the polymer networks by ionic bonding. The hollow poly(MAA/EGDMA)/Fe_3O_4 composite microcapsules showed up to 84.6% loading efficiency of the total DOX. Fig. 7 presents the release profiles of DOX from the hollow poly(MAA/EGDMA)/Fe_3O_4 composite microcapsules at different pH levels over 120 h. The release rate of DOX from the composite microcapsules was pH dependent, where the fraction of DOX released increased as the pH level in the PBS buffer decreased. The release profile of DOX in the acidic solution demonstrates the fast dissociation of poly(MAA/EGDMA)/Fe_3O_4–DOX, and the quantity of the DOX released under acidic conditions was the largest among the three conditions tested (pH levels of 2, 4 and 7) owing to the weaker electrostatic binding between the anionic carboxyl groups and cationic DOX. As a result, the quantity of DOX released under acid conditions was controlled by equilibrating the concentration of the DOX inside the composites and that in the PBS solution. A 43.8% drug release was produced in PBS solution at pH 2. In contrast, lower drug release amounts of 28.0% and 9.5% were released in PBS solutions with pH levels of 4 and 7, respectively. These results suggest that the release of DOX arising from osmotic force was hindered by the strong electrostatic attraction between the cationic DOX and anionic composites.

Conclusion

In summary, we developed a facile synthesis of monodisperse poly(MAA/EGDMA)/Fe_3O_4 composite microcapsules with hollow structures. We suggest that the polymer–metal chelate complexation that occurred in the spherical anionic polymer particles caused the formation of the hollow structures *via* conformational transition. The main strategy for this synthesis is the utilization of the phase separation induced by the formation of relatively hydrophobic regions occurring as a consequence of the interaction between negatively-charged hydrogel chains and positively-charged metal ions. The hollow structures of the poly(MAA/EGDMA)/Fe_3O_4 composite microcapsules were maintained even in a dry state. The magnetic properties of the composite microcapsules were adjusted by control of the medium pH and the concentration of $FeCl_2$ solution used in the synthetic processes. DOX as a model drug was loaded into the microcapsules, and its controlled release behaviors were studied in aqueous solutions with different pH levels. In addition, we confirmed that other metal ions such as $CuSO_4$, $FeCl_3$ and $SnCl_2$ can be used for the synthesis of hollow composite microcapsules. Magnetic hollow poly(MAA/EGDMA) composite microcapsules with pH-responsive properties are a promising material for targeted drug delivery systems and various other applications.

Acknowledgements

This work was supported by the Nano Material Technology Development Program (2012M3A7B4049745) through the National Research Foundation (NRF) funded by the Ministry of Science, ICT and Future Planning.

Notes and references

1 C. Sanchez, B. Julian, P. Belleville and M. Popall, *J. Mater. Chem.*, 2005, **15**, 3559–3592.
2 P. Gupta, K. Vermani and S. Garg, *Drug Discovery Today*, 2002, **7**, 569–579.
3 M. Guo, Y. Yan, H. Zhang, H. Yan, Y. Cao, K. Liu, S. Wan, J. Huang and W. Yue, *J. Mater. Chem.*, 2008, **18**, 5104–5112.
4 Y. Deng, D. Qi, C. Deng, X. Zhang and D. Zhao, *J. Am. Chem. Soc.*, 2008, **130**, 28–29.
5 J. Shin, R. M. Anisur, M. K. Ko, G. H. Im, J. H. Lee and I. S. Lee, *Angew. Chem., Int. Ed.*, 2009, **48**, 321–324.
6 X. Yang, L. Chen, B. Huang, F. Bai and X. Yang, *Polymer*, 2009, **50**, 3556–3563.
7 S. Zeng, K. Tang, T. Li, Z. Liang, D. Wang, Y. Wang and W. Zhou, *J. Phys. Chem. C*, 2007, **111**, 10217–10225.
8 A. Chatzipavlidis, P. Bilalis, L. A. Tziveleka, N. Boukos, C. A. Charitidis and G. Kordas, *Langmuir*, 2013, **29**, 9562–9572.
9 P. Du, J. Zeng, B. Mu and P. Liu, *Mol. Pharmaceutics*, 2013, **10**, 1705–1715.
10 H. S. Lim, E. K. Won, M. Lee, Y. M. Lee and K. D. Suh, *Macromol. Rapid Commun.*, 2013, **34**, 1243–1248.
11 C. Rocchiccioli-Deltche, R. Franck, V. Cabuil and R. Massart, *J. Chem. Res.*, 1987, **5**, 126–127.
12 R. G. C. Moore, S. D. Evans, T. Shen and C. E. C. Hodson, *Phys. E*, 2001, **9**, 9253–9261.
13 F. Bai, B. Huang, X. Yang and W. Huang, *Eur. Polym. J.*, 2007, **43**, 3923–3932.

14 Y. Kim, Y. Park, A. Choi, N. S. Choi, J. Kim, J. Lee, J. H. Ryu, S. M. OH and K. T. lee, *Adv. Mater.*, 2013, **25**, 3045–3049.
15 S. F. Chin, K. S. Iyer and C. L. Raston, *Lab Chip*, 2008, **8**, 439–442.
16 B. Li, H. Cao, J. Shao, M. Qu and J. H. Warner, *J. Mater. Chem.*, 2011, **21**, 5069–5075.
17 X. Yang, X. Zhang, Y. Ma, Y. Huang, Y. Wang and Y. Chen, *J. Mater. Chem.*, 2009, **19**, 2710–2714.
18 J. Berger, M. Reist, J. M. Mayer, O. Felt, N. A. Peppas and R. Gurny, *Eur. J. Pharm. Biopharm.*, 2004, **57**, 19–34.
19 R. Abu-Much, U. Meridor, A. Frydman and A. Gedanken, *J. Phys. Chem. B*, 2006, **110**, 8194–8203.
20 X. Chen, S. Wang, M. Lu, Y. Chen, L. Zhao, W. Li, Q. Yuan, W. Norde and Y. Li, *Biomacromolecules*, 2014, **15**, 2166–2171.
21 Y. Tian, L. Bromberg, S. N. Lin, T. A. Hatton and K. C. Tam, *J. Controlled Release*, 2007, **121**, 137–145.
22 S. Nigam, S. Chandra, D. F. Newgreen, D. Bahadur and Q. Chen, *Langmuir*, 2014, **30**, 1004–1011.
23 G. Minotti, P. Menna, E. Salvatorelli, G. Cairo and L. Gianni, *Pharmacol. Rev.*, 2004, **56**, 185–229.
24 X. J. Kang, Y. Dai, P. Ma, D. Yang, C. Li, Z. Hou, Z. Cheng and J. Lin, *Chem.–Eur. J.*, 2012, **18**, 15676–15682.